JOURNAL OF SOLID STATE CHEMISTRY 72, 234–243 (1988)

Structural Studies of $Li_{0.7}VO_2$ in the Temperature Range 20–300°C

L. P. CARDOSO* AND D. E. COX

Brookhaven National Laboratory, Upton, New York 11973

AND T. A. HEWSTON† AND B. L. CHAMBERLAND

Department of Chemistry, The University of Connecticut, Storrs, Connecticut 06268

Received December 31, 1986; in revised form May 14, 1986

The ordered rock-salt type compound $Li_{0.7}VO_2$ has recently been found to exhibit some unusually large hysteresis effects in its magnetic and thermal properties between 150 and 280°C, related to the magnetic transition known to occur at about 190°C in $LiVO_2$. X-ray and neutron powder diffraction measurements have been made on samples of $Li_{0.7}VO_2$ in an effort to classify structural changes believed to accompany this transition but not hitherto reported in any detail. The unit cell parameters were found to change from $a = 2.837$, $c = 14.775$ Å at 24°C to $a = 2.913$, $c = 14.640$ Å at 263°C, with a large discontinuity in the transition region. Rietveld refinement was carried out on X-ray data collected at these temperatures and on neutron data collected at 35°C, the main change being an increase in the V–O and V–V distances from 1.98 and 2.84 Å at 24°C to 2.02 and 2.91 Å at 263°C, respectively. The only indication of any departure from $R\bar{3}m$ symmetry in the low-temperature phase was the presence of two extremely weak superlattice peaks in the 24°C X-ray data which can be indexed in terms of an enlarged cell with $a' = a\sqrt{3}$, $c' = c$. Above 250°C, the gradual development of a second phase was noted, identified as the cubic spinel LiV_2O_4 resulting from the disproportionation of $Li_{0.7}VO_2$ into $LiVO_2$ and the spinel. Hysteresis effects were observed in the X-ray data which closely parallel those previously reported for the magnetic and thermal properties and which can be attributed to the disproportionation reaction.

Introduction

Li forms a family of oxide compounds with the first-row transition elements of general composition $LiMO_2$, where M can be Sc, Ti, V, Cr, Mn, Fe, Co, and Ni (*1*). These compounds all have structures which are derivatives of rock-salt type, and in the case of $LiVO_2$ the structure is rhombohedral, space group $R\bar{3}m$, with Li and V atoms occupying alternate (111) planes (*2*). $LiVO_2$ is of particular interest insofar as it was found by Bongers (*3*) to undergo a magnetic transition at about 180°C involving a sharp increase in susceptibility on heating, which was later found to coincide with an abrupt discontinuity in the unit cell parameters but no apparent change in the symmetry (*4, 5*). Anomalies in the electrical conductivity were also observed on heating the compound through the transi-

* On leave from Instituto de Fisica, UNICAMP, 13100 Campinas, Sao Paulo, Brazil.

† Present address: Chemistry Division, Naval Weapons Center, China Lake, CA 93555.

0022-4596/88 $3.00

tion (*4, 6*). To explain the magnetic properties, Goodenough (*7*) proposed a mechanism of molecular orbital formation in the basal plane below the transition via the formation of triangular clusters of V atoms, giving a nonmagnetic state with weak Pauli paramagnetism. Unpublished NMR measurements by Löcher and Bongers (*8*) indicated that the V atoms are nonmagnetic below the transition, and that their local symmetry is lower than rhombohedral, consistent with Goodenough's triangular cluster model. They also noted the presence of two very weak lines in the X-ray powder pattern which indicated that the real unit cell of $LiVO_2$ at room temperature has unit cell parameter lattice constants $a' = a\sqrt{3}$ and $c' = c$ with respect to the usual hexagonal parameters. Hewston and Chamberland (*9*) have suggested a model for the phase transition which requires no change in crystallographic symmetry: The low-temperature data are interpreted in terms of a two-dimensional vanadium "metal" cluster layer" formed via covalent-type metal-to-metal bonds. In the high-temperature region, the *d*-electrons become itinerant, leading to in-plane metallic behavior as indicated by high-temperature infrared spectra.

In work aimed at resolving the structure, Hewston and Chamberland (*10*) have described the preparation of single crystals of $LiVO_2$ with two different habits, hexagonal and octahedral. Although the powder patterns of both types were very similar to that of a powder sample prepared by conventional techniques, precession photographs of the hexagonal platelets showed a number of weak superlattice reflections in addition to the strong ones with $R\bar{3}m$ symmetry, consistent with space groups $P6_122$ or $P6_422$ and unit cell parameters $a' = 2a\sqrt{3}$ and $c' = c$.

Differential scanning calorimetric (DSC), thermogravimetric, and magnetic measurements were made on both types of crystals and the powder. An interesting feature of the DSC data for all three materials was that on the first heating cycle a transition was observed at about 260°C, considerably higher than previously reported. On subsequent cooling and heating cycles, a reproducible temperature near 170°C was observed. The magnetic measurements showed the same sort of behavior. The thermogravimetric results showed essentially no weight gain in flowing oxygen below 400°C, a slow increase up to about 750°C, and a rapid increase to saturation between 750 and 800°C. The overall weight gain for all three materials was significantly less than that calculated for oxidation of V^{3+} to V^{5+} and indicated a composition $Li_{0.6-0.7}VO_2$. The Li deficiency is compensated for by the presence of V^{4+} in addition to V^{3+}.

The present paper describes the results of some X-ray and neutron powder diffraction measurements carried out on a similar sample of polycrystalline material from the same batch used in Ref. (*9*) aimed at elucidating the low- and high-temperature structures and the unusual hysteresis behavior described above. While this work was in progress, three papers were published by de Picciotto and co-workers dealing with some structural studies of $LiVO_2$ which had been delithiated by chemical and electrochemical techniques (*11, 12*). In particular, they showed that material of composition $Li_{0.5}VO_2$, which is a two-phase system, transforms irreversibly to the normal spinel LiV_2O_4 at about 300°C, an observation which proved to be very pertinent to some of the results of the present paper.

Experimental Details

A polycrystalline sample of $LiVO_2$ was prepared by solid state reaction of Li_2CO_3 and V_2O_5 in an atmosphere of H_2/Ar as previously described (*9*). The final product was washed with acetic acid to remove un-

reacted Li_2CO_3. It should be noted that exposure of the product to air and/or dilute acids causes the loss of Li ions which result in a nonstoichiometric compound. An X-ray Debye–Scherrer pattern taken with Cu$K\alpha$ radiation showed only a rhombohedral phase with hexagonal unit cell parameters $a = 2.84$ and $c = 14.77$ Å.

Temperature dependence measurements were carried out by both X-ray and neutron diffraction techniques. For the X-ray measurements, the sample was packed into a rectangular depression in a copper sample holder with a resistance heater and thermocouple. The measurements were performed on an automated General Electric XRD5 diffractometer equipped with a fine-focus Cu target and a graphite monochromator in the diffracted beam. Scans were performed over selected angular ranges at 0.04° intervals with Cu$K\beta$ radiation at a variety of temperatures up to 300°C during heating and cooling cycles. With the use of Cu$K\beta$ instead of Cu$K\alpha_1\alpha_2$ radiation, the patterns contain fewer peaks and subsequent data analysis is simplified. Complete data sets for Rietveld refinement were collected in the sequence 24, 263, 130, and 190°C. The average temperature variation during data collection was about 1°C. The actual temperature in the sample was determined in a series of separate experiments on a sample of $LiVO_2$ mixed with MgF_2 which served as an internal standard. The difference between the temperature determined from the unit cell parameters of MgF_2 (*13*) and the indicated temperature was about 5°C less at 300°C.

The neutron measurements were carried out at the Brookhaven High Flux Beam Reactor on a triple-axis diffractometer equipped with a Ge(111) monochromator and a pyrolytic graphite analyzer in the (004) setting. The nominal neutron wavelength was 1.342 Å. The sample was pressed into a pellet about 1 cm in diameter and 1 cm high and mounted in a split-coil resistance furnace. Scans were performed over selected angular ranges at either 0.05° or 0.1° intervals at a variety of temperatures up to 290°C. Complete data sets for use in Rietveld refinements were collected at 35, 264, and 34°C at the end of the cycle.

Results

Temperature Dependence Measurements

X-rays. The four complete data sets collected at 24, 263, 130, and 190°C are shown in Figs. 1a–d. With the exception of a few very weak peaks which will be discussed later, the pattern in Fig. 1a can be indexed in terms of a hexagonal cell with $a = 2.837$ and $c = 14.775$ Å. These values are in good agreement with previously reported values for material of nominal composition $LiVO_2$ except for the c dimensions reported by Kobayasi *et al.* (*4*) and Bongers (*3*), where there is a significant difference (Table I). At 263°C, the rhombohedral symmetry is retained but there are some striking shifts in some of the peak positions (Fig. 1b), with a increasing to 2.913 Å and c decreasing to 14.640 Å, corresponding to a volume increase of about 4.5%. These values agree well with those of Bongers (*3*), but once again there is a large discrepancy with the c dimension reported by Kobayashi *et al.* well in excess of possible experimental uncertainties. It should be noted that a and c appear to change very little with Li content down to $Li_{0.7}VO_2$ (*4*, *11*).

The temperature dependence on the first heating cycle is illustrated in Figs. 2a–d by the evolution of the (018) and (110) reflections, and the corresponding unit cell parameters are indicated by curve I of Fig. 3. There is a small increase in a and c up to 237°C, at which point the start of the transformation is signaled by the appearance of a weak peak between (018) and (110) which is clearly the (110) reflection of the high-temperature phase (Figs. 2c and 2d). Between

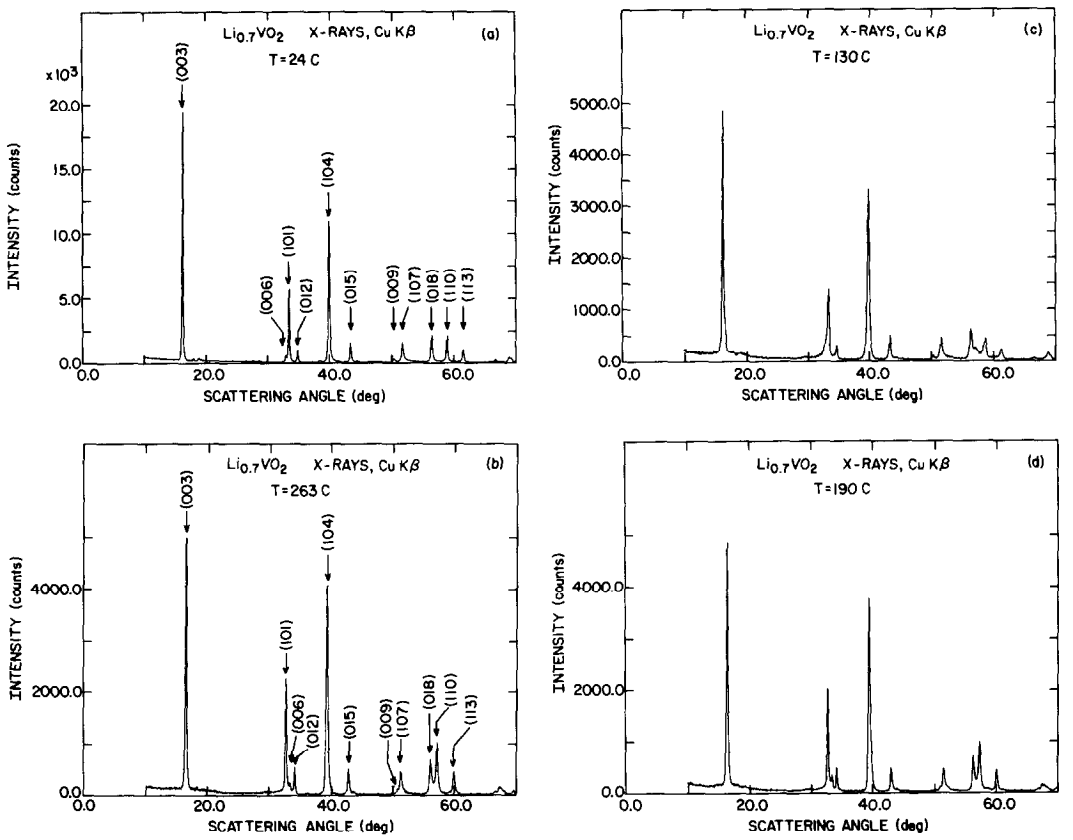

FIG. 1. X-ray powder diffraction scans from $Li_{0.7}VO_2$ obtained with Cu$K\beta$ radiation at various temperatures during heating (24–290°C)—a and b, cooling (290–118°C)—(c), and heating (118–190°C)—(d) cycles. The weak peaks at 18.0, 37.1, and 44.3° are due to a small Cu$K\alpha$ component. Those at 18.8 and 38.2° can be indexed as the (100) and (200) reflections from an $a\sqrt{3}$, c cell.

237 and 264°C, the unit cell parameters undergo a large discontinuous change as shown in Fig. 3, but then change only slightly up to 290°C, the highest temperature reached.

This behavior is not reversible on cooling, however. The high-temperature phase persists down to 170°C, but at 153°C the low-temperature phase finally starts to reappear (Fig. 2e). Rather unexpectedly, however, the high-temperature phase appears to persist down to 118°C (Fig. 2f), the lowest temperature reached on the cooling cycle (curve II in Fig. 3).

The behavior in the second heating cycle

TABLE I

SOME PREVIOUSLY REPORTED UNIT CELL PARAMETERS FOR $LiVO_2$ AT ROOM TEMPERATURE (RT) AND JUST ABOVE THE TRANSITION TEMPERATURE (T_t)

Reference	RT		$>T_t$	
	a(Å)	c(Å)	a(Å)	c(Å)
Bongers (*3*, *5*)	2.845	14.84	2.912	14.65
Petzoldt and Kordes (*14*)	2.845	14.795	—	—
Kobayashi *et al.* (*4*)	2.83	14.87	2.89	14.48
de Picciotto *et al.* (*11*)	2.840	14.785	—	—
Present work	2.837	14.775	2.913	14.640

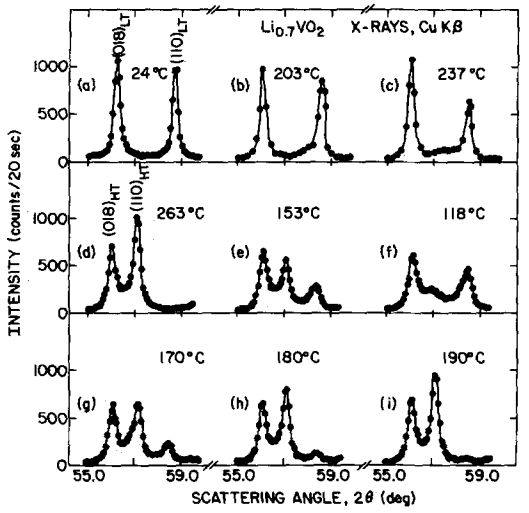

FIG. 2. Evolution of the (018) and (110) reflections from $Li_{0.7}VO_2$ as a function of temperature. Data were obtained with Cu$K\alpha$ radiation.

is quite different from that in the first. The transformation is already underway at 170°C (Fig. 2g) and is complete at 190°C (Figs. 2h and 2i). The corresponding unit cell parameters are shown in curve III of Fig. 3.

Overall, this hysteresis behavior closely parallels the results obtained in the differential scanning calorimetry experiments described in the Introduction (*9*, *10*), namely the observation of a transition at about 260°C on the first heating cycle, at about 155°C on cooling, and at about 175°C on the second heating cycle. The last value corresponds quite closely to the value reported by Bongers (*3*) and Kobayashi *et al.* (*4*).

A detailed examination of the complete pattern obtained at 130°C (Fig. 1c) reveals that in addition to a weak peak first thought to be the (110) reflection of the high-temperature phase, there is a definite asymmetry or shoulder on the high angle side of the $LiVO_3$ (003) reflection at about 17°. A comparison with the data shown in Ref. (*12*) indicates the most likely explanation to be the formation of a small amount of a cubic spinel phase LiV_2O_4 with $a \approx 8.25$ Å, which has strong reflections at these positions, namely (111) and (440).

Figure 1d shows the pattern obtained at 190°C, the final temperature of the second heating cycle. The presence of the spinel phase is now completely masked because of shifts in the $LiVO_2$ peak positions accompanying the transformation to the high-temperature phase.

Three of the very weak peaks present in the patterns in Fig. 1 can be attributed to a small Cu$K\alpha$ component transmitted by the graphite monochromator (i.e., those at 2θ values of 18.0, 37.1, and 44.3°). However, two additional weak reflections are visible in Fig. 1a at about 18.8 and 38.2°. These can be indexed as superlattice reflections with hexagonal indices ($\frac{1}{3}$, $\frac{1}{3}$, 0) and ($\frac{2}{3}$, $\frac{2}{3}$, 0), or (100) and (200) in terms of an enlarged cell

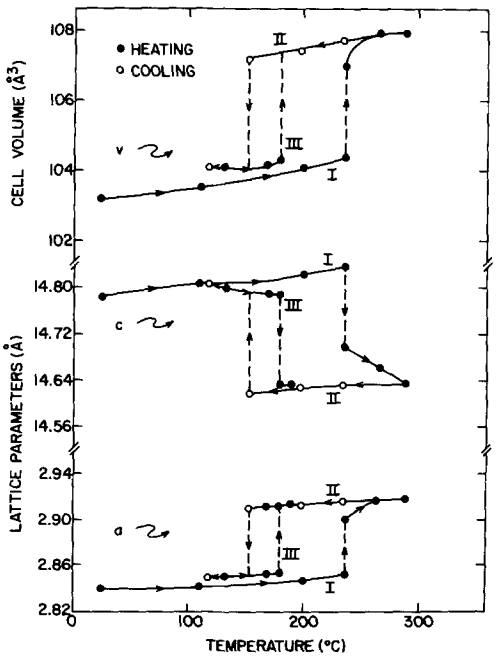

FIG. 3. Variation of unit cell parameters determined from the (018) and (110) reflections as a function of temperature during the first heating cycle (curve I), the first cooling cycle (curve II), and the second heating cycle (curve III).

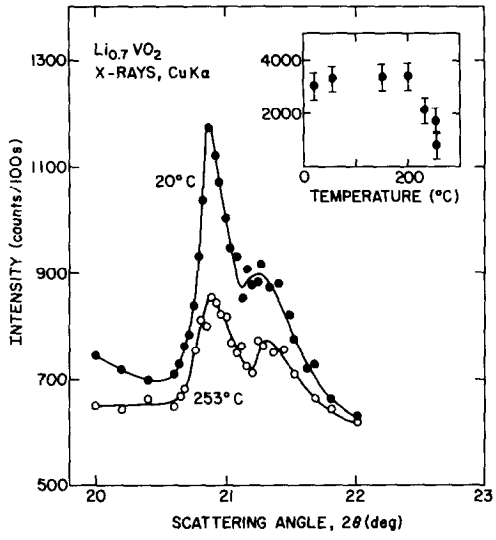

FIG. 4. Scans in the region of the (100) superlattice reflection from $Li_{0.7}VO_2$ obtained with Cu$K\alpha$ radiation at 20 and 253°C. The second peak at 21.3° is an impurity peak, either Li_3VO_4 or Li_2CO_3. The inset shows the integrated intensity of the (100) reflection as a function of temperature.

with unit cell lattice parameters $a\sqrt{3}$, c. These are presumably the two very weak peaks previously noted in Ref. (*8*).

Temperature dependence measurements were carried out on a fresh sample of material for the first of these superlattice reflections. For these measurements Cu$K\alpha$ radiation was used in order to improve the counting statistics. The data obtained at room temperature (Fig. 4) show that there are in fact two peaks. The weaker one at $2\theta = 21.3°$ is believed to be an impurity peak from Li_3VO_4 (*16*) or Li_2CO_3 (*17*). Above 200°C, the integrated intensity falls off quite rapidly as shown in the inset to Fig. 4 and the superlattice peak disappears above the transition at 260°C. This is also evident in Fig. 1b. However, on cooling, this peak did not reappear, although there was an indication of some broad diffuse scattering around the original peak position (Figs. 1c and 1d).

Neutrons. In addition to $LiVO_2$, the neutron scans revealed the present of a significant amount of a second phase identified as Li_2CO_3. This is obviously residual unreacted material remaining after the acetic acid treatment, and is estimated to be about 1% by weight from the relative intensities of the two phases.

As in the case of the X-ray measurements, the (018) and (110) reflections were used to monitor the transformation, as illustrated in Fig. 5. In the initial heating cycle, there is some buildup of diffuse scattering between the two peaks as low as 155°C (Figs. 5a and 5b), which develops into a quite pronounced peak at 232°C (Fig. 5c). At 264°C, the transition appears complete (Fig. 5d) and on cooling there is very little change until 149°C (Fig. 5e), when the low-temperature phase begins to reappear. However, even when the temperature is lowered to 34°C, the scattering in this region is dominated by the third peak at $2\theta = 55.0°$ (Fig. 5f).

This observation and other changes in the pattern are once again consistent with the formation of a second phase with a face-centered cubic cell about 8.25 Å in size. The relative intensities of the two phases indicate that the following disproportion-

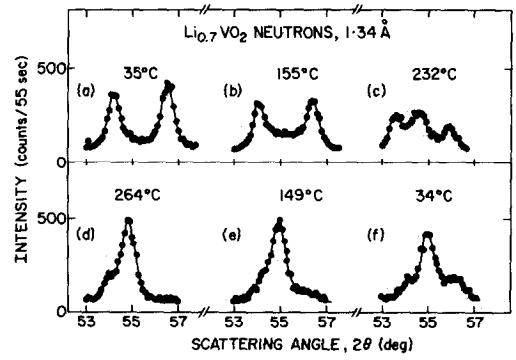

FIG. 5. Evolution of the (018) and (110) reflections from $Li_{0.7}VO_2$ as a function of temperature. Data were obtained with neutrons; wavelength was 1.342 Å.

ation reaction must have occurred on heating:

$$Li_{0.7}VO_2 \rightarrow 0.4\ LiVO_2 + 0.3\ LiV_2O_4.$$

Rietveld Refinement

X-rays

24°C data. Refinement of the room temperature data obtained with Cu$K\beta$ radiation was carried out with a local version of the Rietveld program (*18*) in which the peak shapes are described by the pseudo-Voigt function, which is an approximation to the convolution of Lorentzian and Gaussian functions (*19, 20*). The Gaussian half-widths (FWHM) are given by the usual expression

$$T_G = (U \tan^2 \theta + V \tan \theta + W)^{1/2}$$

and the Lorentzian half-widths by

$$T_L = X \tan \theta + Y/\cos \theta,$$

where U, V, W, X, and Y are refinable parameters (*21*). Background was estimated by interpolation between values determined at a number of points between the peaks, and the contribution from a given reflection was taken out to five times the FWHM on either side of the peak position.

In the initial stages of refinement a total of 11 parameters were varied—the oxygen positional parameter z, the unit cell parameters a and c, individual isotropic temperature factors for the three atoms, a zero point correction, a scale factor, and three half-width parameters, W, X, and Y. The refinement converged to R values of 0.075 for R_I and 0.188 for R_{WP}, compared to the "expected" value R_E of 0.081, corresponding to a goodness-of-fit index $S^2 = (R_{WP}/R_E)^2$ of 5.4. The final values are listed in Table II, column I, and an interesting result is the rather high value obtained for the B of vanadium compared to that of oxygen, 1.6 Å^2 against 0.5 Å^2.

Some additional refinements were carried out at this point. A small improvement was obtained by including the half-width parameter U as a variable, but a considerably greater improvement was obtained by assigning anisotropic temperature factors B_{11} and B_{33} to vanadium, as permitted by the symmetry. The results of this refinement are listed in column II of Table II, and indicate a substantially larger amplitude of vibration for vanadium in the basal plane.

Attempts to vary the occupation factor of Li were inconclusive, but the relatively high B value of 3 Å^2 is not inconsistent with some Li deficiency.

263°C data. Refinement of the 263°C data was carried out along similar lines, and the final results are listed in Table II, column III. Once again, the fit is noticeably improved by the assignment of anisotropic temperature factors to the vanadium, but now the results indicate a substantially larger vibrational amplitude along the c axis. In addition, there is significant broadening of the peaks, particularly at higher angles, as shown by the large increase in the Gaussian half-width parameter U and a smaller increase in the Lorentzian parameter Y.

Neutrons

35°C data. Rietveld refinement of the data set collected from a virgin sample at 35°C was carried out in a manner analogous to that described above. The contribution from a given reflection was taken over a total range of 3 FWHM, and regions corresponding to the Li_2CO_3 impurity were excluded from the refinement. The three Gaussian half-width parameters, U, V, and W were refined, and individual isotropic temperature factors were assigned to Li and O. Since vanadium is a very weak scatterer for neutrons, its temperature factor was constrained to be equal to that of O. In the later stages of refinement, a noticeable improvement was obtained when anisotropic temperature factors were assigned to

TABLE II

RESULTS FROM RIETVELD REFINEMENT OF X-RAY AND NEUTRON DATA FOR $LiVO_2$ FOR VARIOUS MODELS AS DESCRIBED IN TEXT

	X-Rays (Cu$K\beta$)			Neutrons (1.342 Å)	
	24°C		263°C	35°C	
	I	II	III	IV	V
O : z	0.2418(2)	0.2418(2)	0.2432(3)	0.2430(1)	0.2425(1)
Li : B(Å^2)	3.1(4)	3.0(3)	0.5(4)	2.5(2)	0.5(2)
V : B	1.56(4)	—	—	0.59	0.59
V : B_{11}	—	1.93(5)	0.56(5)	—	—
V : B_{33}	—	0.79(6)	2.2(1)	—	—
O : B(Å^2)	0.46(7)	0.34(6)	0.3(1)	—	—
O : B_{11}(Å^2)	—	—	—	0.31(3)	0.44(3)
O : B_{33}(Å^2)	—	—	—	1.10(7)	1.16(7)
Li : f	1.0	1.0	1.0	1.0	0.72(1)
a(Å)	2.8374(1)	2.8373(1)	2.9132(2)	2.8307(3)	2.8307(3)
c(Å)	14.7747(9)	14.7734(7)	14.6404(17)	14.7165(19)	14.7161(18)
U(deg^2)	—	0.046(8)	0.244(25)	4.68(19)	4.25(19)
V(deg^2)	—	—	—	−3.04(19)	−2.61(18)
W(deg^2)	0.022(1)	0.020(1)	0.022(2)	0.71(4)	0.62(4)
X(deg)	0.324(8)	0.26(1)	0.22(3)	—	—
Y(deg)	0.016(3)	0.028(3)	0.062(8)	—	—
R_I	0.075	0.053	0.054	0.072	0.057
R_{WP}	0.188	0.175	0.227	0.161	0.153
R_E	0.081	0.082	0.109	0.121	0.121
S^2	5.4	4.6	4.3	1.8	1.6

Note. Space group $R\bar{3}m$, Li in 3(a) at 0, 0, 0; V in 3(b) at 0, 0, 0.5; O in 6(c) at 0, 0, z. Neutral atom scattering factors were used for the X-ray refinements. Neutron scattering amplitudes were taken as −0.203, −0.038, and 0.581 × 10^{-12} cm for Li, V, and O, respectively. The unit cell parameters from the X-ray and neutron refinements at room temperature differ because of a small error in the neutron wavelength of about 0.3%. f is the Li occupancy factor. The e.s.d.'s are given in parentheses and referred to the least significant digit(s).

O, with the results shown in column IV of Table II. A further improvement was obtained when the occupation factor of Li was allowed to vary, with the final results listed in column V of Table II. The value of 0.72 found for the Li content is in good agreement with the figure determined from the thermogravimetric analysis (*10*) and confirms the defect nature of the virgin material. The profile fit and difference plot for the neutron refinement are shown in Fig. 6.

Discussion

The diffraction results presented above closely parallel the results obtained for the magnetic and thermal behavior described in Ref. (10), and confirm the Li-deficient nature of the starting phase. The disproportionation of the material between 250 and 300°C complements the results obtained by de Picciotto and Thackeray (*12*) on the transformation of chemically delithiated

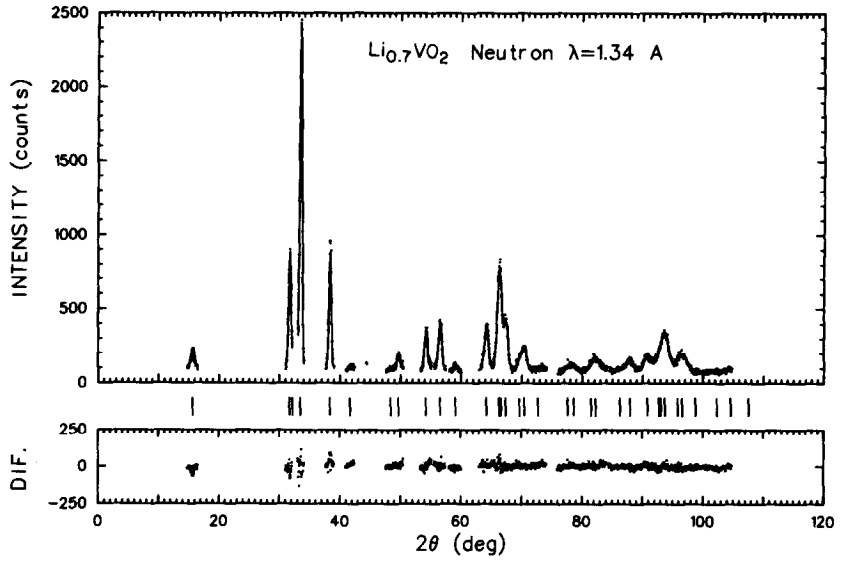

FIG. 6. Profile fit and difference plot for $Li_{0.7}VO_2$ neutron data at 35°C. Short vertical markers represent allowed reflections. Data in the vicinity of the Li_2CO_3 impurity peaks were excluded from the refinement.

samples of $Li_{0.5}VO_2$ to the spinel phase LiV_2O_4. It seems clear that the origin of the large hysteresis effects previously observed (*10*) is this disproportionation reaction. The transition between 170 and 190°C observed during the second heating cycle is quite close to the value reported by Bongers (*3*) for the presumed stoichiometric compound, and can therefore be attributed to $LiVO_2$ produced in the disproportionation reaction. It is interesting to note, however, that the transformation temperature of the virgin material is about 70°C higher.

Unfortunately, the complications introduced by the appearance of the spinel phase make it impossible to carry out as detailed a structural analysis as originally planned. The results of the Rietveld analysis in Table II for the two rhombohedral phases do not differ much except for the unit cell parameters, the principal change being increases in the V–V and V–O distances of 0.07 and 0.04 Å, respectively (Table III). The observation of two very weak peaks which can be indexed as the (100) and (200) reflections from an $a\sqrt{3}$, c cell agrees with the remark made in Ref. (*8*), and would indicate that the symmetry of room temperature $Li_{0.7}VO_2$ is lower than $R\bar{3}m$, but the data are obviously inadequate for a detailed analysis. However, if the triangular cluster model illustrated in Ref. (*5*) is assumed, the intensities of these two superlattice reflections can be accounted for qualitatively by a shift in the V positions of about 0.1 Å, with the Li and O atoms fixed in their ideal $R\bar{3}m$ positions. The much larger value of the in-plane anisotropic temperature factor for V obtained in the X-ray

TABLE III

SELECTED INTERATOMIC DISTANCES IN $LiVO_2$

	X-rays		Neutrons
	24°C	263°C	35°C
V–V (Å)	2.837	2.913	2.837
V–O (Å)	1.979	2.021	1.984
Li–O (Å)	2.124	2.138	2.118

refinement of the 24°C data (Table II) is consistent with static displacements of this magnitude. A reasonable choice of space group would be $P31m$. However, it is not clear why long-range order is not reestablished after heating the virgin sample above the transition and cooling again to room temperature, and the present result may not rule out the symmetrical metal cluster-layer model suggested in Ref. (*9*) since experimental data are lacking on pure stoichiometric $LiVO_2$. The very weak superstructure reflections seen in virgin $Li_{0.7}VO_2$ may be related to Li^+/vacancy and/or V^{4+}/V^{3+} ordering within the planes—they would therefore not be observed after disproportionation to the spinel phase and stoichiometric $LiVO_2$.

Further work is still needed to understand the details of the phase transformation in $LiVO_2$, but it appears unlikely that this can be accomplished with conventional powder diffraction techniques.

Acknowledgments

The work carried out at Brookhaven National Laboratory was supported by the Division of Materials Sciences, U.S. Department of Energy, under Contract DE-AC02-76CH00016. One of the authors (L.P.C.) was supported in part by Conselho Nacional de Desenvolimento Cientifico e Tecnologico-CNPq, Brazil.

References

1. T. A. Hewston and B. L. Chamberland, *J. Phys. Chem. Solids* **48,** 97 (1987), and references therein.
2. W. Rudorff and H. Becker, *Z. Naturforsch. B* **9,** 613 and 614 (1954).
3. P. F. Bongers, Ph.D. dissertation, University of Leiden (1957).
4. S. Kobayashi, K. Kosuge, and S. Kachi, *Mater. Res. Bull.* **4,** 95 (1969).
5. P. F. Bongers, "Crystal Structure and Chemical Bonding in Inorganic Chemistry" (C. J. M. Rooymans and A. Rabenau, Eds.), Chap. 4, North-Holland, Amsterdam (1975).
6. B. Reuter, R. Weber, and J. Jaskowski, *Z. Elektrochem.* **66,** 832 (1962).
7. J. B. Goodenough, "Magnetism and the Chemical Bond," Interscience, New York (1963).
8. P. R. Locher and P. F. Bongers, private communications.
9. T. A. Hewston and B. L. Chamberland, *J. Solid State Chem.* **65,** 100 (1986).
10. T. A. Hewston and B. L. Chamberland, *J. Solid State Chem.* **59,** 168 (1985).
11. L. A. de Picciotto, M. M. Thackeray, W. I. F. David, P. G. Bruce, and J. B. Goodenough, *Mater. Res. Bull.* **19,** 1497 (1984).
12. L. A. de Picciotto and M. M. Thackeray, *Mater. Res. Bull.* **20,** 187 (1987); L. A. de Picciotto and M. M. Thackeray, *Solid State Ionics* **18–19,** 773 (1986).
13. Y. S. Touloukian and C. Y. Ho, Eds., "Thermophysical Properties of Matter," Vol. 13, p. 1042, Plenum, New York (1977).
14. J. Petzoldt and E. Kordes, *Z. Anorg. Allgem. Chem.* **338,** 69 (1965).
15. K. Vidyasagar and J. Gopalakrishnan, *J. Solid State Chem.* **42,** 217 (1982).
16. A. R. West and F. P. Glasser, *J. Solid State Chem.* **4,** 20 (1972).
17. H. E. Swanson, H. F. McMurdie, M. C. Morris, and E. H. Evans, "Standard X-ray Diffraction Powder Patterns," National Bureau of Standards Monograph 25, Section 8, p. 42 (1970).
18. H. M. Rietveld, *J. Appl. Crystallogr.* **2,** 65 (1969).
19. R. A. Young and D. B. Wiles, *J. Appl. Crystallogr.* **15,** 430 (1982).
20. G. K. Wertheim, M. A. Butler, K. W. West, and D. N. E. Buchanan, *Rev. Sci. Instrum.* **45,** 1369 (1974).
21. D. E. Cox, *Acta Crystallogr. Sect. A* **40,** Suppl. C369 (1984).